Available online at www.sciencedirect.com
ScienceDirect
Journal of Magnetic Resonance 182 (2006) 49–54
JMR Journal of Magnetic Resonance
www.elsevier.com/locate/jmr

Spin 3/2 Zeeman perturbed NQR in the presence of slow sample rotation

R.P. Panguluri [1], B.H. Suits *

Physics Department, Michigan Technological University, Houghton, MI, USA

Received 20 April 2006; revised 7 June 2006
Available online 27 June 2006

Abstract

Theoretical and experimental results are presented for the case of Zeeman perturbed nuclear quadrupole resonance (NQR) using spin-3/2 nuclei with a small Zeeman interaction, γB_0, while the sample is very slowly rotated. It is found that the decay envelope for a simple two-pulse echo measurement can be strongly affected even though the sample may rotate only a few degrees or less during the course of the measurement. To lowest order the decay envelope can be described using a one dimensional function of the product of γB_0, the rotation rate, and the square of the pulse spacing. Aside from an indirect and weak dependence on the quadrupole asymmetry parameter, η, the result is independent of the NQR frequency. Identical results are expected for a stationary sample in a small rotating magnetic field. The effect seen here may be used to advantage to measure rotational motion, for example of particles in fluids, or may be an additional complication for some Zeeman perturbed NQR measurements, including some NQR detection and imaging methods.

Keywords: NQR; Sample rotation; Beats; Zeeman perturbed; Slow rotation

1. Introduction

Several nuclear magnetic resonance (NMR) pulse techniques have been developed to observe motion of liquids and solid particles [1–3]. These techniques are principally sensitive to translational motion of the molecules. In many cases, knowledge of rotational motion, such as the motion of a solid particle suspended in a fluid which undergoes non-laminar flow, is of interest and provides useful information about the turbulence of the fluid. In addition, the measurements using a sample undergoing other types of motion, such as a transverse vibration, can be expected to show similar effects. With those possible future applications in mind, we undertook a study of the effects of a simple well-defined (slow) rotation on a nuclear quadrupole resonance (NQR) signal.

Several groups have observed that relatively slow physical rotation (~1 Hz) of a sample during some magnetic resonance experiments can have a significant effect, most notably on the measured spin–lattice relaxation time, T_1 [4,5]. Hill and Yesinowski [6] used slow rotation of a severely quadrupole broadened ^{14}N NMR spectrum to enhance the signal to noise ratio and at the same time obtain information about the quadrupole coupling. In that measurement, the excitation bandwidth is small compared to the line width and the slow rotation continuously brings "fresh spins" (spins not recently excited) into the measurement window due to the time-dependent quadrupole perturbation. The time dependence of the Hamiltonian during a simple echo measurement gives rise to an echo decay envelope which depends on the quadrupole broadening. More rapid rotational motion has been observed by Esteve et al. [7] who investigated the effects of rotational Brownian motion of polystyrene spheres and showed that

* Corresponding author. Fax: +1 906 487 2933.
E-mail address: suits@mtu.edu (B.H. Suits).
[1] Present address: Department of Physics and Astronomy, Wayne State University, Detroit, MI 48201, USA.

1090-7807/$ - see front matter © 2006 Elsevier Inc. All rights reserved.
doi:10.1016/j.jmr.2006.06.008

the resulting nuclear dipole relaxation provides a means to study that motion. Tycko [8] investigated very fast rotation (1–4 kHz) for a pure NQR measurement and observed a spectral splitting associated with Berry's phase.

Here the effects of slow rotational motion (0–15 Hz) on the measurement of a Zeeman perturbed nuclear quadrupole resonance (NQR) measurement for a nuclear spin $I = 3/2$ in a polycrystalline ("powder") sample is studied. The experiment is similar to the quadrupole perturbed NMR measurements of Hill et al. [6] except the roles of the Zeeman and quadrupole interactions are reversed.

It is noted that some recently developed NQR techniques involving time-dependent magnetic fields produced by permanent magnets in motion [9] may produce a result akin to what is described here if those techniques are applied to spin-3/2 nuclei. In addition, several NQR imaging techniques have been proposed which use magnetic field gradients [10]. The results reported here shown that even slow or seemingly inconsequential sample motion during such a measurement could significantly affect the image contrast.

We start with a description of the theory followed by experimental observations and a comparison of those observations with theory.

2. Theory

The Hamiltonian in the laboratory reference frame without sample rotation can be written

$$\boldsymbol{H} = \boldsymbol{R}^{-1}\boldsymbol{H}'_{\boldsymbol{Q}}\boldsymbol{R} + \boldsymbol{H}_z, \tag{1}$$

where primes are used to designate the quadrupole principal axes coordinates, $\boldsymbol{R}$ is a rotation operator which transforms between the principal axes and the laboratory frame, and

$$\begin{aligned} \boldsymbol{H}'_{\boldsymbol{Q}} &= A\left(3\boldsymbol{I}_{z'}^2 - \boldsymbol{I}^2 + \eta\left(\boldsymbol{I}_{x'}^2 - \boldsymbol{I}_{y'}^2\right)\right) \\ \boldsymbol{H}_z &= -\gamma B_0 \boldsymbol{I}_z. \end{aligned} \tag{2}$$

Here $A = e^2qQ/(4I(2I-1))$ is the overall strength of the electric quadrupole interaction, η is the asymmetry parameter ($0 \leqslant \eta \leqslant 1$), and $\boldsymbol{H}_z$ represents the Zeeman interaction for a nucleus with spin I and gyromagnetic ratio γ, in the presence of a magnetic field B_0 applied along the z-axis of the laboratory reference frame.

With sample rotation at an angular frequency, ω_r, about the x-axis, this becomes

$$\boldsymbol{H} = \boldsymbol{Q}^{-1}\boldsymbol{R}^{-1}\boldsymbol{H}'_{\boldsymbol{Q}}\boldsymbol{R}\boldsymbol{Q} + \boldsymbol{H}_z, \tag{3}$$

where $\boldsymbol{Q} = e^{i\omega_r t \boldsymbol{I}_x}$ and $\boldsymbol{R}$ is the appropriate coordinate transformation at $t = 0$. In the principle axes coordinates this can be written

$$\boldsymbol{H}' = \boldsymbol{H}'_{\boldsymbol{Q}} + \boldsymbol{R}\boldsymbol{Q}\boldsymbol{H}_z\boldsymbol{Q}^{-1}\boldsymbol{R}^{-1}. \tag{4}$$

If the rotation is slow, that is $\omega_r t \ll 1$ for times of relevance (e.g., $t \leqslant T_2$), we can expand $\boldsymbol{Q}$ and use the usual angular momentum commutation relations to write this as

$$\boldsymbol{H}'(t) = \boldsymbol{H}'(0) + \gamma B_0 \boldsymbol{R}\left(\omega_r t \boldsymbol{I}_y - \frac{1}{2}\omega_r^2 t^2 \boldsymbol{I}_z + \ldots\right)\boldsymbol{R}^{-1}. \tag{5}$$

Transforming back to the laboratory frame, where measurements are made, this is

$$\boldsymbol{H}(t) = \left(\boldsymbol{R}^{-1}\boldsymbol{H}'_{\boldsymbol{Q}}(0)\boldsymbol{R} + \gamma B_0 \boldsymbol{I}_z\right) + \left(\omega_r t \boldsymbol{I}_y - \frac{1}{2}\omega_r^2 t^2 \boldsymbol{I}_z + \ldots\right), \tag{6}$$

where the first set of parentheses is the Hamiltonian for a static Zeeman perturbed NQR experiment, and the second a time-dependent magnetic field. For the experiments described below, the sample will have rotated a maximum of about 2° during the measurements and hence the second term corresponds to a small time-dependent perturbation. The corrections to the equation of motion which arise due to the fact that the rotating frame is a non-inertial reference frame are negligible here. In addition, the adiabatic approximation is good and will be used for the relatively slow motion described. That is, the time-dependent perturbation simply gives rise to time-dependent energy levels and transition frequencies.

Here, we restrict the discussion to nuclei with spin $I = 3/2$ and to cases where the Zeeman contribution to the energy is small compared to the electric quadrupole coupling. The strategy will be to diagonalize the static part of the Hamiltonian, then use the wavefunctions obtained and perturbation theory to obtain the time-dependent energy levels and the expected (Hahn echo) signal for different relative orientations of the static field and applied RF field. The result will be averaged over all orientations (i.e., all $\boldsymbol{R}$) numerically. Before proceeding with the details, however, it is worth pointing out some general conclusions already evident.

First, if the rotation is made about the direction of the magnetic field (the z-axis), then the time-dependent perturbation vanishes and one would then expect to see no effect due to rotation if the approximations used here are valid. Second, since spin-3/2 nuclear wavefunctions in the absence of an applied field depend only on the quadrupole asymmetry parameter, η, and with the applied field they can then be determined quite accurately using degenerate perturbation theory [11], the resulting time-dependent perturbation may depend on η but otherwise should not depend on the NQR frequency. Third, if we can truncate the expansion of the time-dependent perturbation after the first term, then the resulting additional accumulated phase evolution of the wavefunction due to rotation will be proportional to t^2. Hence, for a simple two-pulse echo experiment with pulse spacing τ, an appropriate dimensionless parameter to describe the effects of the rotation on the echo amplitude is $\gamma B_0 \omega_r \tau^2$. That is, the shape of the decay envelope due to the rotational motion will depend only on η and $\gamma B_0 \omega_r \tau^2$ and is independent of which spin-3/2 nucleus is used and the strength of the electric quadrupole interaction, A. This is somewhat of

a remarkable conclusion, demonstrated experimentally below, since the experiment we are actually describing involves rotating the electric field gradient, keeping the magnetic field fixed.

For a spin 3/2 nucleus in an electric quadrupole field and in the absence of a magnetic field, there will be two pairs of degenerate energy levels with energies $E_4 = E_3 = -E_2 = -E_1 = h\nu_Q\rho/2$ where $\nu_Q/6 = A$ and $\rho = (1+\eta^2/3)^{1/2}$ [11]. Defining $\sin\delta = [(\rho-1)/(2\rho)]^{1/2}$ the wavefunctions can be written using bra-ket notation in the principal axis reference frame as

$$\begin{aligned}
|4_0\rangle &= \cos\delta|-3/2\rangle + \sin\delta|1/2\rangle \\
|3_0\rangle &= \cos\delta|3/2\rangle + \sin\delta|-1/2\rangle \\
|2_0\rangle &= \cos\delta|-1/2\rangle - \sin\delta|3/2\rangle \\
|1_0\rangle &= \cos\delta|1/2\rangle - \sin\delta|-3/2\rangle.
\end{aligned} \tag{7}$$

In the presence of a small magnetic field of magnitude B_0 with x, y, and z components B_x, B_y, and B_z in the principal axis frame, the energy levels found using degenerate perturbation theory are [11]

$$\begin{aligned}
E_{4,3} &= \frac{h\nu_Q\rho}{2} \pm \frac{\gamma h}{4\pi\rho}\left[(\rho-1+\eta)^2B_x^2 + (\rho-1-\eta)^2B_y^2 + (2+\rho)^2B_z^2\right]^{1/2} \\
E_{2,1} &= \frac{-h\nu_Q\rho}{2} \pm \frac{\gamma h}{4\pi\rho}\left[(\rho+1-\eta)^2B_x^2 + (\rho+1+\eta)^2B_y^2 + (2-\rho)^2B_z^2\right]^{1/2},
\end{aligned} \tag{8}$$

where the + signs go with the even levels, and the minus signs with the odd levels. Hence there will be four closely spaced transitions. The corresponding wavefunctions we derived can be written

$$\begin{aligned}
|4\rangle &= \cos(\theta/2)|4_0\rangle + e^{i\varphi}\sin(\theta/2)|3_0\rangle \\
|3\rangle &= \cos(\theta/2)|3_0\rangle - e^{-i\varphi}\sin(\theta/2)|4_0\rangle \\
|2\rangle &= \cos(\theta'/2)|2_0\rangle + e^{i\varphi'}\sin(\theta'/2)|1_0\rangle \\
|1\rangle &= \cos(\theta'/2)|1_0\rangle - e^{-i\varphi'}\sin(\theta'/2)|2_0\rangle,
\end{aligned} \tag{9}$$

where

$$\begin{aligned}
\cos\theta &= \frac{(2+\rho)B_z}{\left((2+\rho)^2B_z^2 + (\rho-1+\eta)^2B_x^2 + (\rho-1-\eta)^2B_y^2\right)^{1/2}} \\
\cos\theta' &= \frac{(2\rho-1)B_z}{\left((2\rho-1)^2B_z^2 + (\rho+1-\eta)^2B_x^2 + (\rho+1+\eta)^2B_y^2\right)^{1/2}} \\
\tan\varphi &= \frac{\rho-1-\eta}{\rho-1+\eta}\frac{B_y}{B_x}; \quad \tan\varphi' = -\frac{\rho+1+\eta}{\rho+1-\eta}\frac{B_y}{B_x}.
\end{aligned} \tag{10}$$

In practice one must be careful when computing φ and φ' to ensure the result is in the correct quadrant.

Using these wavefunctions and the usual derivation of an on-resonance echo signal along an arbitrary direction "s" in the principal axis system following two excitations spaced a time τ apart along that same direction one finds a contribution to the signal in the absence of rotation which can be written

$$S_s \propto \sin^2\xi_2 \sin 2\xi_1 \sum_{\substack{k=1,2\\ j=3,4}} \frac{|I_{kj}|^4}{\Omega_1^3}\cos\omega_{jk}(t-\tau), \tag{11}$$

where

$$\begin{aligned}
I_{kj} &= \langle k|\boldsymbol{I}_s|j\rangle \\
\Omega_1 &= \left(|I_{13}|^2 + |I_{23}|^2\right)^{1/2} \\
\omega_{jk} &= (E_j - E_k)/\hbar \\
\xi_i &= \gamma B_1\Omega_1 t_i
\end{aligned} \tag{12}$$

where $\boldsymbol{I}_s$ is the component of the angular momentum operator along s, B_1 is the strength of the RF magnetic field used for excitation, and t_i is the duration of the i-th pulse. For a powder, one should then average over all directions, s.

Now, to include the time dependence for slow rotation in the adiabatic approximation, we simply write

$$\omega_{jk}(t) = \omega_{jk}(0) + \lambda_{jk}t \tag{13}$$

and follow through the derivation above. Keeping track of the accumulated phase shifts and evaluating at $t = \tau$, the cosine in the summation of Eq. (11) is then replaced with $\cos(\lambda_{jk}\tau^2)$.

Now the problem is to determine λ_{jk}. Here, we use RF excitation and detection along a laboratory x-axis and B_0 applied along the laboratory frame z-axis. Then λ_{jk} is found using Eq. (8) above and three Euler angles, (α,β,γ), relating the laboratory frame and the principal axis frame at $t = 0$. With a rotation rate ω_r and assuming that $\omega_r t \ll 1$ for all times of relevance one gets that $\lambda_{jk} = (dE_j/dt - dE_k/dt)/\hbar$ where

$$\begin{aligned}
\frac{dE_{4,3}}{dt} &= \pm\omega_r\frac{\pi h\gamma B_0}{\rho}\frac{(\rho-1+\eta)^2c_xd_x + (\rho-1-\eta)^2c_yd_y + (2+\rho)^2c_zd_z}{\left((\rho-1+\eta)c_x^2 + (\rho-1-\eta)^2c_y^2 + (2+\rho)^2c_z^2\right)^{1/2}} \\
\frac{E_{2,1}}{dt} &= \pm\omega_r\frac{\pi h\gamma B_0}{\rho}\frac{(\rho+1-\eta)^2c_xd_x + (\rho+1+\eta)^2c_yd_y + (2-\rho)^2c_zd_z}{\left((\rho+1-\eta)c_x^2 + (\rho+1+\eta)^2c_y^2 + (2-\rho)^2c_z^2\right)^{1/2}}
\end{aligned} \tag{14}$$

where, the plus sign is for the even and the minus for the odd levels, and

$$\begin{aligned}
c_z &= \cos\beta & d_z &= \sin\beta\sin\gamma \\
c_x &= \sin\beta\cos\alpha & d_x &= -\cos\alpha\cos\beta\sin\gamma - \sin\alpha\cos\gamma \\
c_y &= \sin\beta\sin\alpha & d_y &= -\sin\alpha\cos\beta\sin\gamma + \cos\alpha\cos\gamma.
\end{aligned} \tag{15}$$

Since virtually every term in the result has a very complicated angular dependence, the powder average over the Euler angles was calculated numerically. Such calculations are significantly simpler for the axially symmetric case of $\eta = 0$.

3. Experiment

The results from two different samples with $\eta \approx 0$ are presented here in detail: Cs_2ZnBr_4, and p-dichlorobenzene ($C_6H_4Cl_2$). All measurements were made at room tempera-

ture. The Cs_2ZnBr_4 was prepared as described in Ref. [12] and has six different Br NQR resonances which are observable [13,14]. Here we use the ^{79}Br ($\gamma = 6.711 \times 10^7\ s^{-1}\ T^{-1}$) resonance at 68.98 MHz which has the shortest spin–lattice relaxation time, $T_1 = 16$ ms, and lowest temperature coefficient. For our sample this line is inhomogeneously broadened with a FWHM of about 70 kHz and exhibits a spin–spin relaxation time, T_2, measured using a Hahn echo, of 96 and 400 μs in Earth's field and in magnetic fields greater than about 10 G, respectively. This resonance has been assumed to correspond to $\eta \approx 0$ [15] which we verified by looking at the powder line shape in the presence of a magnetic field parallel to the RF coil axis [16,17]. The *p*-dichlorobenzene was obtained from a local merchant (sold as "Moth Flakes") and was ground into a fine powder. The ^{35}Cl resonance ($\gamma = 2.621 \times 10^7\ s^{-1}\ T^{-1}$) near 34.27 MHz was used, which had a line width of just under 1 kHz. For *p*-dichlorobenzene at room temperature, $T_1 = 25$ ms, $T_2 = 0.7$ ms, and $\eta \approx 0.07$ [18,19].

The geometry used is illustrated in Fig. 1. The probe used for the initial experiments was a modified home-built NMR probe where a small d.c. motor was added at the end of the probe away from the sample and a long mechanical shaft and right angle gears were coupled to the sample container. Once the effect was seen, including verification that rotation about an axis along the field direction had little effect, a dedicated set-up was constructed using a speed-stabilized motor and reduction gearing, and a long non-magnetic shaft into a shielded Al enclosure which contained the RF coil and tuning components. Rotational rates (0–15 Hz) are stable and accurate to better than 0.1% for most measurements and to better than 1% at the slower rates. All components were firmly mounted on a non-magnetic table for convenient positioning of the sample in the stray field of an 89 mm bore, 8.5 T superconducting magnet. The motor is approximately 1 m farther from the magnet where the field was no more than a few gauss at its strongest. The magnetic field at the sample location was measured using a hand-held gaussmeter. To help ensure a uniform RF magnetic field during excitation, the RF coil used was approximately twice as long as, and twice the diameter of, the sample container.

All measurements shown use a two-pulse spin echo, where the second pulse is twice the length of the first (i.e., nominally a π/2–π Hahn echo), with appropriate phase cycling for coherent signal averaging. The pulse lengths were set by maximizing the echo signal at the peak of the resonance in zero magnetic field. To remove the effects of "slow beats," [20] which for the data shown here are much smaller and much more rapid than the effects due to rotation, and the decay due to relaxation, the amplitude of the spin echo is measured twice for each data point—with the motor on, $S(\omega)$, and with it off, $S(0)$. The ratio, $S(\omega)/S(0)$, of the two measurements is reported here, and hence includes only the changes of the echo envelope due to the effects of rotation. In the absence of an applied magnetic field (i.e., $B_0 < 1$ G) $S(\omega)/S(0) = 1$, within experimental error, for both samples for the range of rotation rates used here.

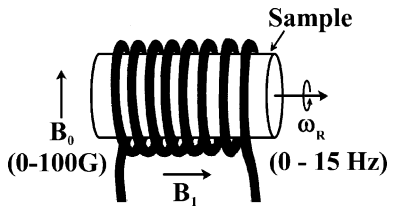

Fig. 1. The geometry used for these measurements.

4. Results and discussion

Fig. 2 shows the theoretical results for $\eta = 0$, where the "pulse lengths" $\gamma B_1 t_1$ and $\gamma B_1 t_2 = 2\gamma B_1 t_1$ were adjusted to obtain the maximum (theoretical) echo signal in the absence of rotation, corresponding to what was done in the experiments. The full calculation is shown, plus also results of separate calculations for the inner transitions and outer transitions, for reasons discussed below. Fig. 3 is a combined plot including data at $B_0 = 36$ G for *p*-dichlorobenzene and 10 G for Cs_2ZnBr_4 under a variety of conditions. It can be seen that the use of $\gamma B_0 \omega_r \tau^2$ as the single (unitless) parameter works quite well and there is reasonable agreement with the theory. This is quite satisfying given the fact that the measurements included different compounds, different nuclei, and that one NQR line had significant inhomogeneous broadening while the other did not.

Two different situations were found where the theory did not work well: some measurements at very low magnetic

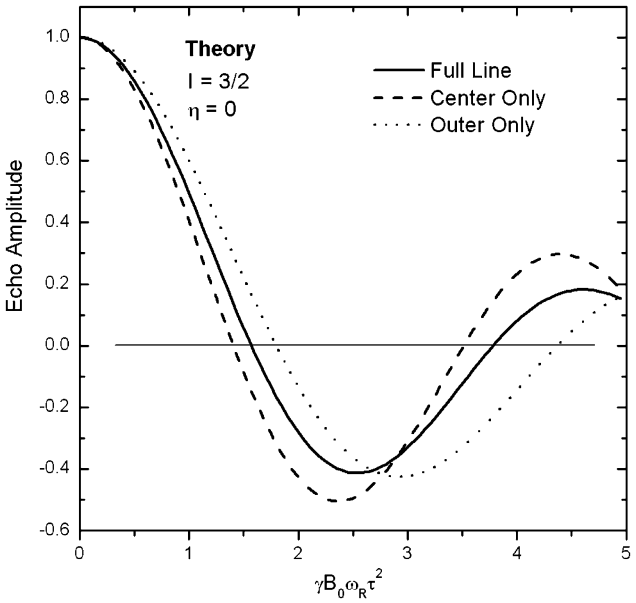

Fig. 2. Theoretical results for the two-pulse echo decay envelope as a function of the dimensionless parameter $\gamma B_0 \omega_r \tau^2$.

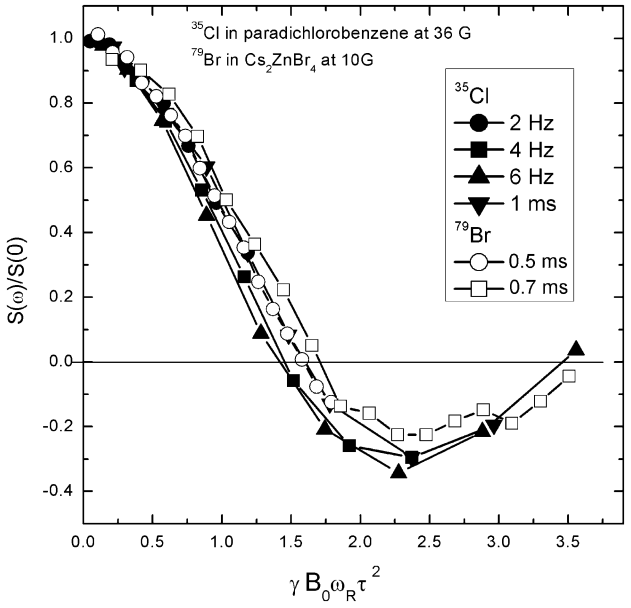

Fig. 3. Combined data for two different samples under a variety of conditions in low magnetic fields. The caption indicates the value of the parameter which is kept constant, either τ or ω_r, while the other was swept. The solid lines connecting the points are a guide for the eye.

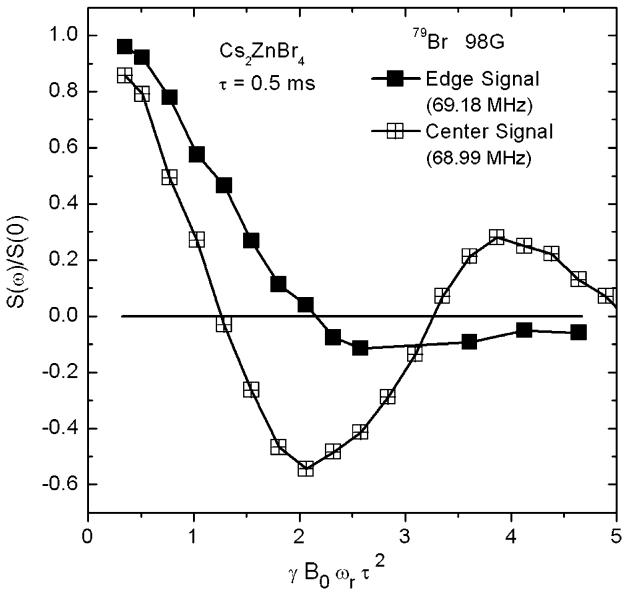

Fig. 4. Data for one sample in a larger magnetic field with the RF carrier at the center frequency of the powder pattern and near one edge of the powder pattern. The solid lines connecting the points are a guide for the eye.

fields (<10 G) with long echo delays and most measurements at higher magnetic fields (>50 G). In both cases, we believe this is because assumptions made when deriving the theory were not satisfied in the experiment.

The T_2 relaxation observed for spin-3/2 NQR in the absence of a magnetic field is often significantly shorter than in the presence of a magnetic field. This is a well-known effect related to the degeneracy which is lifted when a field is applied—that is, "like spins" become "unlike" or "semi-like spins." The effect depends on orientation, of course. In weaker magnetic fields a significant number of nuclei will be oriented so they have only a very small Zeeman interaction and hence will have the faster T_2 of "like spins." Those with a stronger Zeeman interaction will have a longer T_2. This distribution of T_2's can then create an effective preferential orientation of the sample for longer echo delay times.

In larger fields, there simply is not enough excitation bandwidth to excite all the transitions. Fig. 4 shows data from one sample in a field of 98 G for two different RF carrier frequencies. Clearly there is a significant difference. The two frequencies shown in Fig. 4 correspond to the center of the spectrum and a shoulder near the edge of the powder pattern. While a complete calculation for this limited excitation would be formidable, a crude approximation to this situation is possible. By keeping only the terms with $k = 1$, $j = 3$, and $k = 2, j = 4$, in Eq. (11) only the center section of the powder pattern is involved. Likewise, keeping only terms with $k = 1, j = 4$, or $k = 2, j = 3$, only the outermost set transitions will be included. These two situations are included in Fig. 2. It can be seen that at least qualitatively, the behavior of the data is similar, in particular if one looks at the position of the first zero crossing.

The results obtained using the larger magnetic fields suggest that one could formulate a 2-d spectroscopy based on this technique. In its crudest form, the 2-d data would be collected with one dimension being the RF carrier frequency and the other being $\gamma B_0 \omega_r \tau^2$. While such an experiment is beyond the scope of this work, the possibility that it may provide an alternate method to accurately extract a value for η is under study.

It is also noted that the shape of the decay envelope will depend somewhat on the pulse lengths used. In addition, only rotations along the same axis as the detection were considered here for practical reasons, but a qualitatively similar, though quantitatively different, result should be expected if this orientation is changed, for example so that the excitation/detection, the applied magnetic field, and the rotation axes are mutually orthogonal.

5. Conclusions

Theoretical and experimental results are presented for the case of Zeeman perturbed nuclear quadrupole resonance (NQR) using spin 3/2 nuclei with a small Zeeman interaction, γB_0, while the sample is very slowly rotated. It was found that the decay envelope for a simple two-pulse echo measurement can be strongly affected even though the sample may rotate a few degrees or less during the course of the measurement. The echo decay envelope can be described using a one dimensional function of the product $\gamma B_0 \omega_r \tau^2$. For small magnetic fields, the result is independent of which nucleus is used and, aside from a weak dependence on the quadrupole asymmetry parameter, η, is independent of the NQR frequency. Identical results are expected for a stationary sample in a small rotating

magnetic field. For larger magnetic fields, limited excitation bandwidth can significantly affect the results.

Acknowledgment

Portions of this work were supported by NRL Broad Agency Announcement Grant N00173-01-1-G000.

References

[1] K.J. Packer, The study of slow coherent molecular motion by pulsed nuclear magnetic resonance, Mol. Phys. 17 (1969) 355–368.
[2] M.A. Hemminga, P.A. de Jager, The study of flow by pulsed nuclear magnetic resonance. II. Measurement of flow velocities using a repetitive pulse method, J. Magn. Reson. 37 (1980) 1–16.
[3] J.R. Suryan, Nuclear resonance in flowing liquids, Proc. Indian Acad. Sci. Sect. A 33 (1951) 107–111.
[4] D.E. Woessner, H.S. Gutowsky, Spin exchange and spin–lattice relaxation induced by mechanical rotation of solids, J. Chem. Phys. 29 (1958) 804–812.
[5] R. Eckman, Enhanced nuclear spin lattice relaxation of deuterium in solids by sample rotation, J. Chem. Phys. 79 (1983) 524–525.
[6] E.A. Hill, J.P. Yesinowski, A slow-turning method for measuring large anisotropic interactions in inhomogeneously broadened nuclear magnetic resonance spectra, J. Chem. Phys. 106 (1997) 8650–8659.
[7] D. Esteve, C. Urbina, M. Goldman, H. Frisby, H. Raynaud, L. Strzelecki, Direct observation of rotational Brownian motion of spheres by NMR, Phys. Rev. Lett. 52 (1984) 1180–1183.
[8] R. Tycko, Adiabatic rotational splittings and Berry's phase in nuclear quadrupole resonance, Phys. Rev. Lett. 58 (1987) 2281–2284.
[9] J. Luznik, J. Pirnat, Z. Trontelj, Polarization enhanced ^{14}N NQR detection with a nonhomogeneous magnetic field, Solid State Commun. 121 (2002) 653–656.
[10] H. Robert, P.J. Prado, Threat localization in QR explosive detection systems, Appl. Magn. Reson. 25 (2004) 395–410, and references therein.
[11] H.R. Brooker, R.B. Creel, Zeeman nuclear quadrupole resonance line shapes in powders ($I = 3/2$), J. Chem. Phys. 61 (1974) 3658–3664, and references therein.
[12] H. Nakayama, N. Nakamura, H. Chihara, ^{81}Br nuclear quadrupole resonance of Cs_2ZnBr_4 and crystal stability of compounds of A_2MX_4 type, Bull. Chem. Soc. Jpn 60 (1987) 99–103.
[13] S. Plesko, R. Kind, H. Arend, New structural phase sequence with incommensurate phases in A_2BX_4 halides with β-K_2SO_4 structure, Phys. State Solid (a) 61 (1980) 87–94.
[14] I.S. Kovaleva, I.Ya. Kuznetsova, V.A. Fedorov, A.A. Boguslavskii, R.Sh. Lotfullin, The preparation and NQR study of the compounds of the $ZnBr_2$-CsBr system, Russ. J. Inorg. Chem. 35 (1990) 100–103.
[15] D.E. Scaife, Halogen nuclear quadrupole resonance in tetrahedral halo complexes of zinc, Aust. J. Chem. 24 (1971) 1315–1323.
[16] N. Sunitha Bai, N. Reddy, R. Ramachandran, Zeeman-perturbed spin–echo FT NQR spectroscopy, J. Magn. Reson. A 102 (1993) 137–143.
[17] O. Ege, S. Hamai, H. Negita, Powder Zeeman NQR study on the absorption forms for a nuclear spin of 3/2: dependence on the angle between the directions of an oscillating magnetic field and a static magnetic field, and observation of large η, J. Mol. Struct. 345 (1995) 139–144.
[18] A.H. Brunetti, ^{35}Cl nuclear quadrupole spin–lattice relaxation in paradichlorobenzene, J. Phys. C: Solid State 10 (1977) 617–621.
[19] D.E. Woessner, H.S. Gutowsky, Pure nuclear quadrupole relaxation and its temperature dependence in solids, J. Chem. Phys. 39 (1963) 440–456.
[20] M. Bloom, "Slow Beats" in nuclear quadrupole induction, Phys. Rev. 94 (1955) 1396–1397.